MACROJOURNALS

The Journal of **Macro**Trends in Technology and Innovation

Sensitivity analysis of a winding system with unwinding-idle-winding rollers for steel plate

Yonghui Park*, Kyutae Park, Sungyuen Won, Wankee Hong, Myeongsik Cheon, and Hyunchul Park
*POSTECH, Korea**

Abstract

To wind a rolled steel plate, precise winding process is necessary with proper winding tension and speed. Rotational motions had been considered as a primary interest about stress distributions and tension control. However, elasticity of the steel plate is sufficiently stiff to interact with planar motions of adjacent rollers as a spring-damper. We develop a mathematical model of the winding process in steel production. The model considers the winder, idle roller, and unwinder. This model extends a previous winding model that describes the web material. The suggested model includes planar motions with bearing stiffness of each roller. Compared to the previous model, the strip tension is extremely high, so the bearings should be very stiff to maintain constant tension. Based on the model, the effects of strip slip and eccentricity of the unwinder, and the pre-tension force required to maintain a coil are investigated by reviewing dynamic behaviors. This model can be used to check unusual vibrational data of the roller and coil statues about stress distributions, tension, and coiled length. Especially, bearing stiffness, slip on the idle roller, and eccentric mass on the unwinder makes additional peak frequencies; 397.6 Hz, 4.5 Hz corresponding slip-ratio, and 2.502 Hz corresponding rotational speed & radius of the unwinder respectively.

Keywords: *winding system, unwinding-idle-winding rollers, steel plate*

1. Introduction

Rolling is a process in which metal stock is compressed by passing it through one or more pairs of cylindrical rollers to reduce it to target thickness, then wrapped around a cylindrical winder. During this process the stock (slab) is subjecting to a reciprocating motion between winders. For rolling process to be successful, forward and backward tension on the strip are very important. The tension is generally determined by the rotation speed of the roller and controller, and can affect a coil state on the winder. The magnitude of the tension affects the rotary component that

interacts with the strip. Most research about winding has focused on internal stress in the coil [1-4]. However, the internal stress is highly related to the strip tension [5], so development of a robust winding system requires understanding of the mechanisms of winding in a transferring system that includes a winder and roller.

Generally, the winding system consists of an unwinder, an idle roller, and a winder; the components are connected by a tensioned strip. When the roller rotates with different angular velocity of each roller, different tension of each strip span occurs. Research about the winding system has primarily considered the web material. Based on the basic theorem for the winding [6], various models were suggested about roller controller, unusual cases of surface, slip, and temperature variation, and so on. For instance, mathematical models of tension between relative spans [7], relations between control roll force and winding roll Wound In Tension [8] were developed, and proportional-integral-differential (PID) control and Nonlinear PID control of winding [9] were compared. All of these studies considered distinct web motions, but Newton's laws, mass conversion, and momentum conversion have been used to represent tension and mass variation between each pair of rollers [10-12].

We extend a previous torsional model of the winding system that can be used to describe winding process of the steel strip from previous research [10]. The previous model was based on a state-space model and did not include non-linear terms [13-14]; the model presented here includes linearized forms of all non-linear terms; these include strip length, radius, and inertia moment variations. The model has 12 degrees of freedom (df). Each roller has 3 df, that are possible in planar motion. The model also features automatic calculation of the position and orientation of the rotary component and strip. Especially, we distinguish two points of contact in the idle roller, because planar motions of the roller cause the tangential velocity of the steel strip to vary, so tangential and normal forces on the roller also vary. Lastly, we add a spiral spring model to represent the coil on the unwinder and on the winder.

2. Torsional winding system

The 3-span winding system (Fig 1) includes an unwinder, two idle rollers, and a winder. The unwinder and winder can each be regarded as a combination of the roller itself and the steel coil that accumulates on it. Each roller has its own motor to maintain constant angular velocity and to tension on the strip; to ensure that the motor accomplishes these tasks, it is governed by a PID controller. We organize equations of motion that describe translational coordinates s_1, s_2, s_3, s_4 of the strip (Eq. 1), instead of rotational coordinates θ_1, θ_2, θ_3, θ_4 about the roller, which cannot express slip between the roller and strip.

$$\begin{aligned}
&\frac{d}{dt}\left(\frac{J_1}{r_1}\dot{r}_1\right) \quad -T_{fric1}+T_1 r_1\\
&\frac{d}{dt}\left(\dot{r}_2 \quad \frac{J_2}{r_2}\right) \quad -\frac{r_2}{J_2}T_{fric2}+\left(T_2-T_1\right)\frac{r_2^{\,2}}{J_2}\\
&\frac{d}{dt}\left(\dot{r}_3 \quad \frac{J_3}{r_3}\right) \quad -\frac{r_3}{J_3}T_{fric3}+\left(T_3-T_3\right)\frac{r_3^{\,2}}{J_3}\\
&\frac{d}{dt}\left(\frac{J_4}{r_4}\dot{r}_4\right) \quad -T_{fric4}-T_3 r_4
\end{aligned} \tag{1}$$

During the winding process, radius of the unwinder and winder are changed by the coil accumulation. To account for these variations, we define radius variation of the unwinder and winder (Eq. 2), length variation of the span (Eq. 3), inertia variation of the coil (Eq. 4), and tension variation of the strip span (Eq. 5) [10, 15].

$$\begin{aligned}
&\frac{dr_1}{dt}=\frac{-h}{2\pi r_1}v_1\\
&\frac{dr_2}{dt},\frac{dr_3}{dt}=0\\
&\frac{dr_4}{dt}=\frac{h}{2\pi r_4}v_4
\end{aligned} \tag{2}$$

$$\begin{aligned}
&\frac{dL_1}{dt}=\frac{r_1-r_2}{L_1}\frac{dr_1}{dt}\\
&\frac{dL_2}{dt}=0\\
&\frac{dL_3}{dt}=-\frac{r_3-r_4}{L_3}\frac{dr_4}{dt}
\end{aligned} \tag{3}$$

$$J_i=\frac{1}{2}\pi\times\rho\times\left(r_i\right)^4\times W \qquad \left(i=1,2,3,4\right) \tag{4}$$

$$\frac{dT_k}{dt}=\frac{1}{L_k}\left(EA-T_k\right)v_{k+1}-\frac{1}{L_k}\left(EA-T_{k-1}\right)v_k+\frac{1}{L_k}\left(EA-T_k\right)\frac{dL_k}{dt} \qquad \left(k=1,2,3\right) \tag{5}$$

During numerical iteration, MATLAB code calculates a high-order time derivative of the each physical quantity, and applies the Taylor series to estimate the radius, length, inertia, and tension in the current step [16].

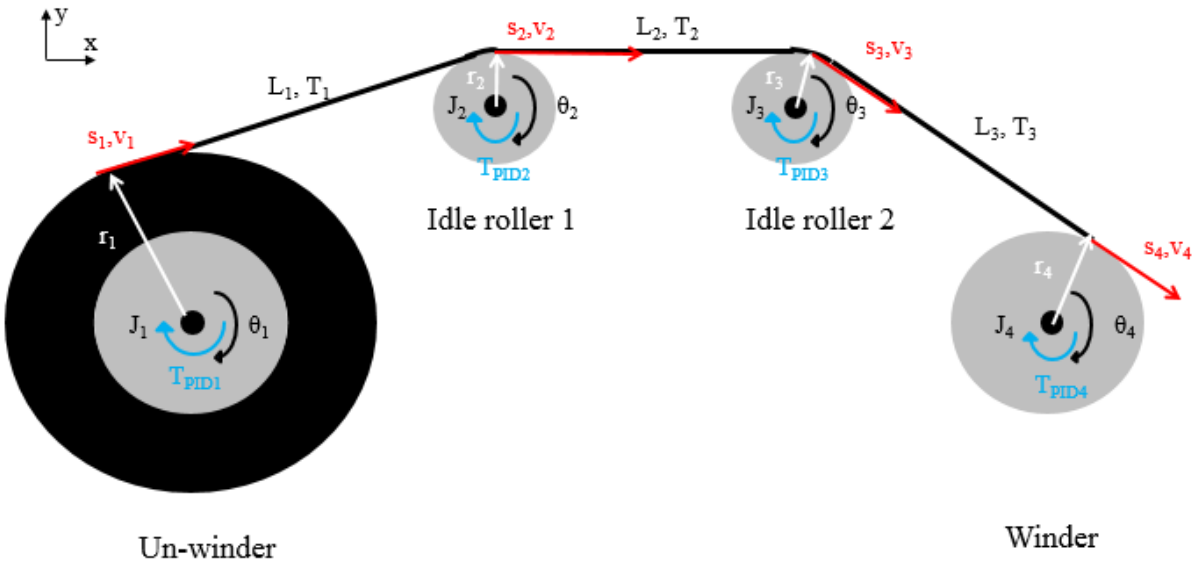

Fig. 1. Torsional model of the 3-spans winding system for strip winding

3. Model development

3.1 Planar winding system

The torsional model covers the physical quantities of Eq. (2)-(5) with pinned condition at the center of each roller, but we should consider geometrical information about translational and rotational motions. Therefore, the planar model includes the translational motion of the center of each roller. The center of each roller is mounted on a bearing, which can move in the horizontal (*x*) and vertical (*y*) directions (Fig. 2).

The model includes code to calculate how *x*,*y* motions of the roller affect each strip span's length and contact pressure angle (Eqs. 6-7).

$$\begin{aligned} m_i \ddot{\quad} &\quad \dot{\quad} \quad \dot{\quad} \quad \dot{\quad} \quad - x_{i-initial}) + N_{x,i} \\ m_i \ddot{\quad} &\quad \dot{\quad} \quad \dot{\quad} \quad \dot{\quad} \quad - y_{i-initial}) + N_{y,i} \end{aligned} \quad (i = 1,2,3,4) \tag{6}$$

$$L_k^{\ 2} = L_{c,k}^{\ 2} + (r_k - r_{k+1})^2 \qquad (k = 1,2,3) \tag{7}$$

Eq. (7) can be converted by time derivative as Eq. (8), not Eq. (3).

$$2L_k \frac{dL_k}{dt} = 2L_{c,k} \frac{dL_{c,k}}{dt} + 2(r_k - r_{k+1}) \frac{dr_k}{dt} + 2(r_k - r_{k+1}) \frac{-dr_{k+1}}{dt} \qquad (k = 1,2,3) \tag{8}$$

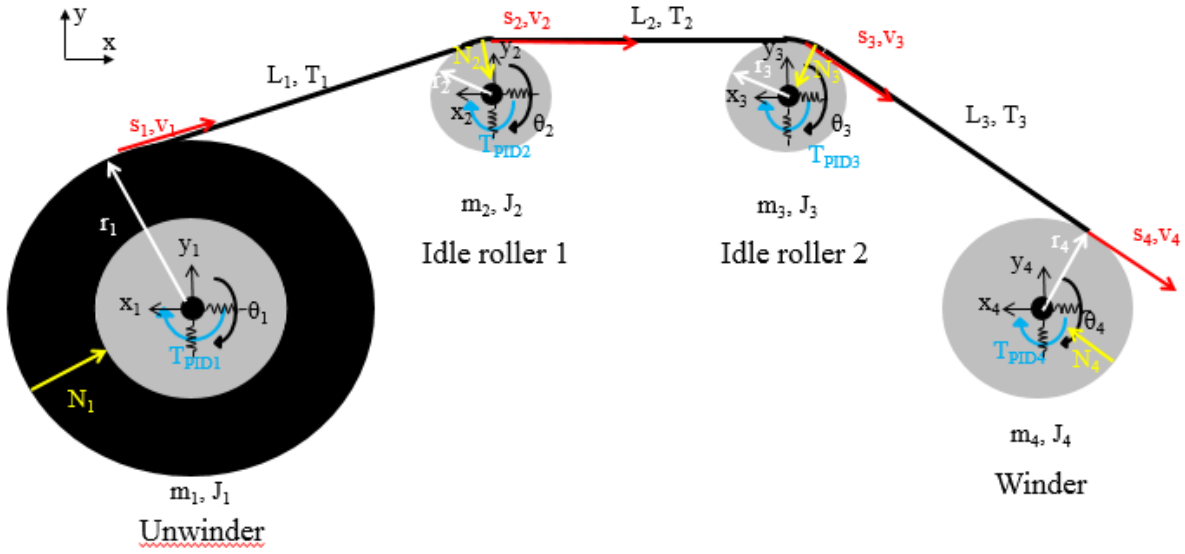

Fig. 2. Planar model including bearings of the three spans for steel plate

The tangential velocity at the edge of the roller varies according to the df (Fig. 3). The torsional model has homogeneous tangential velocity regardless of angular position. However, tangential velocity changes according to the position of the roller's center (Eq. 9). As a result, the tangential velocity of the strip varies among contact positions on the roller. This difference affects the tension, so we include this effect in every numeric iteration.

$$v = r\dot{\theta} \qquad \sqrt{(\dot{x}\ \ \ )^2 + (\dot{y}\ \ \ )^2} \tag{9}$$

Eq. (10) calculates the contact pressure angle on the idle roller (Fig. 4).

$$\theta_{1,j} = \tan^{-1}\left(\frac{|x_j - x_{j+1}|}{|y_j - y_{j+1}|}\right)$$
$$\theta_{2,j} = \tan^{-1}\left(\frac{|x_{j+1} - x_{j+2}|}{|y_{j+1} - y_{j+2}|}\right) \longrightarrow \theta_{contact,j} = \left(\pi - \theta_{1,j} - \theta_{2,j} - \theta_{3,j} - \theta_{4,j}\right) \quad (j = 1,2) \qquad (10)$$
$$\theta_{3,j} = \cos^{-1}\left(\frac{L_j}{L_{c,j}}\right)$$
$$\theta_{4,j} = \cos^{-1}\left(\frac{L_{j+1}}{L_{cj+1}}\right)$$

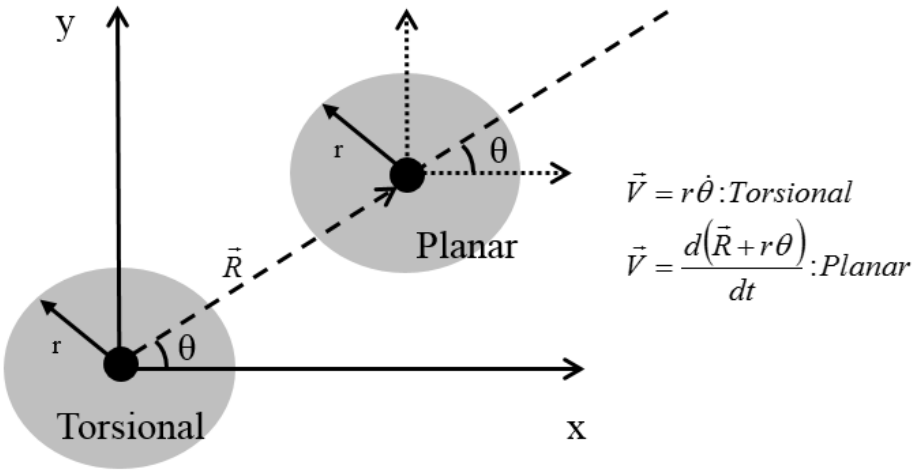

Fig. 3. Effect of center motion on tangential velocity on the outer edge of the roller.

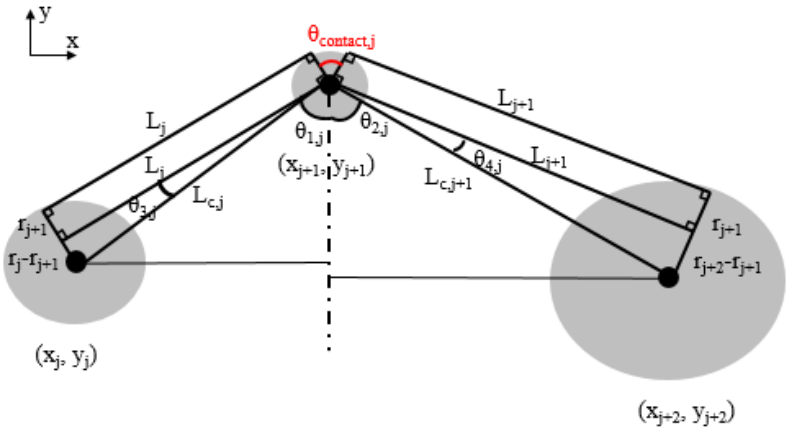

Fig. 4. Contact angle between the steel strip and rollers at the idle roller

3.2 Effects of friction and eccentricity of the unwinder and the winder

The strip can slip on the roller during winding, but the previous model ignored this phenomenon, i.e. relative motions between the roller and the strip were assumed to be constant. To realize strip slip, we must consider additional force equilibriums. In the previous model the dynamic frictional force was treated as a damping element, and static frictional force was compensated for by adjusting motor torque [13, 14]. This characteristic comes from the proportional relationship between the frictional force and angular velocity of the roller (Eq. 11). We add translational coordinates of the strip on the roller for the slip and derived equations of motion and force equilibriums (Eq. 12). If $coeff_i$ = 1 (i = 1 – 4), the corresponding strip and roller do not slip.

$$T_{fric,i} = \frac{B_i}{r_i} v_i \qquad (i = 1,2,3,4) \tag{11}$$

$$\frac{d}{dt}\left(\frac{J_1}{r_1}\dot{\theta}_1\right) = -T_{fric1} + F_{fric,plate,1} r_1$$

$$\frac{d}{dt}\left(\frac{r_2}{J_2}\dot{\theta}_2\right) = -\frac{r_2}{J_2} T_{fric2} + F_{fric,plate,2} \frac{r_2^2}{J_2}$$

$$\frac{d}{dt}\left(\frac{r_3}{J_3}\dot{\theta}_3\right) = -\frac{r_3}{J_3} T_{fric3} + F_{fric,plate,3} \frac{r_3^2}{J_3}$$

$$\frac{d}{dt}\left(\frac{J_4}{r_4}\dot{\theta}_4\right) = -T_{fric4} - F_{fric,plate,4} r_4$$

$$\begin{aligned}
&\frac{d}{dt}\left(m_{plate,1}v_{plate,1}\right) = T_1 - F_{fric,plate,1}\\
&\frac{d}{dt}\left(m_{plate,2}v_{plate,2}\right) = T_2 - T_1 - F_{fric,plate,2}\\
&\frac{d}{dt}\left(m_{plate,3}v_{plate,3}\right) = T_3 - T_2 - F_{fric,plate,3}\\
&\frac{d}{dt}\left(m_{plate,4}v_{plate,4}\right) = -T_3 - F_{fric,plate,4}\\
&\begin{pmatrix}
F_{fric,plate,1} = T_1 \times coeff_1\\
F_{fric,plate,2} = \left(T_2 - T_1\right) \times coeff_2\\
F_{fric,plate,3} = \left(T_3 - T_2\right) \times coeff_3\\
F_{fric,plate,4} = -T_3 \times coeff_4
\end{pmatrix}
\end{aligned} \tag{12}$$

We also consider the possible eccentricity of the strip coil; this situation occur when the coil slips internally. Generally, the motion has no slip when all internal and external forces (e.g., winding tension, bending moment, friction) are in equilibrium. However, maintaining constant winding tension is a difficult task. Moreover, variable winding tension (i.e., the taper tension pattern), has been applied during processing of in winding web material to improve the quality of the product [17]. Therefore, we define an eccentric mass to represent non-homogeneous rotation of the unwinder or winder and to represent the eccentric force that comes from rotation, and that affects translational motion (Eq. 13).

$$\begin{aligned}
Fx_{ecc,ii} &= m_{ecc,ii}\omega_{ii}^{\,2} r_{ecc,ii}\cos\omega_{ii}t\\
Fy_{ecc,ii} &= m_{ecc,ii}\omega_{ii}^{\,2} r_{ecc,ii}\sin\omega_{ii}t \qquad \left(ii = 1,4\right)
\end{aligned} \tag{13}$$

3.3 Pre-tension force on the strip coil

The web material has low elasticity, but the steel strip must be subjected to high tension to maintain its curvature. Without tension, the steel strip comes loose, the layers do not contact each other, and the coil loses symmetry. Bending moment on the spring can be estimated by considering the coil that is fixed on the roller (Fig. 5). When bending moment *M* is applied, the coil is under compression and high frictional force occurs at contact layers that meet in a coil shape. To realize the coiling mechanism, we apply a spiral spring theory that calculates tangential force between initial and current coil shape of the unwinder and winder. After applying bending moment *M*; deformed, the coil can maintain its coil shape by tangential tension *T*. In contrast to a spiral spring, the steel plate has elasticity that changes with the length

of the coil (Eq. 14-16) [18].

$$\alpha = \frac{12 \times 180 \times M \times L}{\pi \times E \times b \times t^3} \tag{14}$$

$$k = \frac{\pi \times E \times b \times t^3}{12 \times 180 \times L} \tag{15}$$

$$L = \pi \times n \times \left(R_e + R_i \right) = \frac{\pi \left(R_e^{\,2} - R_i^{\,2} \right)}{a + t} \tag{16}$$

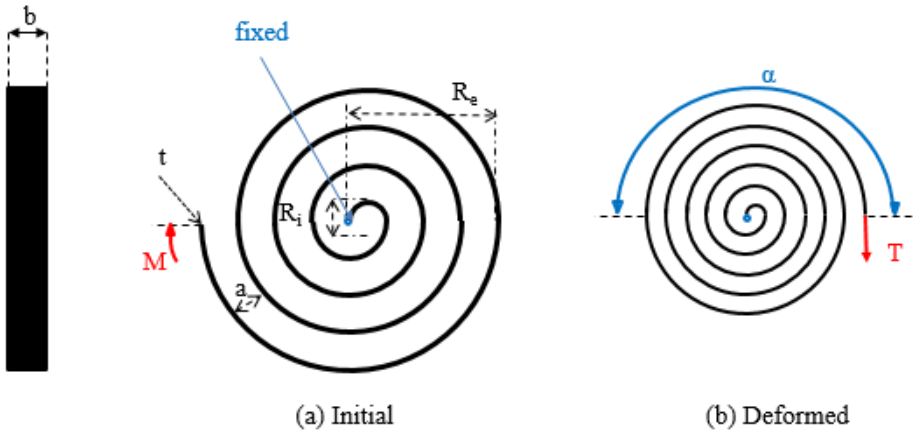

Fig. 5. Bending moment on a spiral spring with fixed inner end of the spring

3.4 Design variables and simulation conditions

The two models were compared under specified design variables (Table 1) and simulation conditions (Table 2). In simulations conditions, the unwinder, idle roller 1, idle roller 2, and winder all rotate with tangential velocity 200 m/min, and slip is assume to not occur.

Table 1. Design variables of the three-span winding system

Quantity	Value	Quantity	Value
Elasticity of the strip	200 GPa	Initial radius of $r_1/r_2/r_3/r_4$	0.8/0.2/0.2/0.424 m
Width of the strip	1 m	Initial tension of L_1 & L_2 & L_3	50 ton
Thickness of the strip	1 mm	Initial inertia of moment of the unwinder, idle roller 1, idle roller 2, and winder	5134.3 / 20.0559 / 20.0559 / 405.1223 kg·m^2
Density of the strip	7980 kg/m^3	Initial mass of the unwinder, idle roller 1, idle roller 2, and winder	16045 / 1002.8 / 1002.8 / 4507 kg
Damping coefficient B_i (i=1,2,3,4)	10^6 N·s/m	P/I/D gain	10^9/0/0
Bearing stiffness	10^{10} or 10^{16} N/m		

Table 2. Conditions for simulation of three-span winding system

Quantity	Value
Tangential velocity of unwinder, idle roller 1, idle roller 2, and winder	200 mpm
Slip coefficient	1/0.9999/0.9999/1 or 1/0.8/0.8/1
Radius of the eccentric mass	$r_{ecc}=r_{1,i}/2$
Pre-coiled layer	376

4. Results and Discussion

4.1 Dynamic characteristic comparison between torsional and planar model.

The torsional and planar model respond differently to the strip tension and length (Fig. 6). When the bearing stiffness is high, the models differ only in their predictions of local vibrations, which result from the stiffness of the bearings. However, when the bearing stiffness is low, the tension profile is very sensitive to planar motions of the rollers. The strip tension between idle roller 1 and idle roller 2 can even be negative when the bearing stiffness is 10^{10} N/m.

To investigate relation between the bearing and tension, the strip tension between the unwinder and idle roller 1, and *x*-*y*-ϑ displacement of the unwinder were subjected to Fourier transform (Fig. 7). The tension and planar motions both showed a 397.6-Hz peak frequency that is the natural frequency of the bearing. Additionally, we the inlet and outlet velocity of the strip contact on the roller showed distinct tangential velocities when the bearing stiffness decreased. Consequently, the differences in Fig. 6 result from velocity difference on the contact area as a consequence of the planar motions.

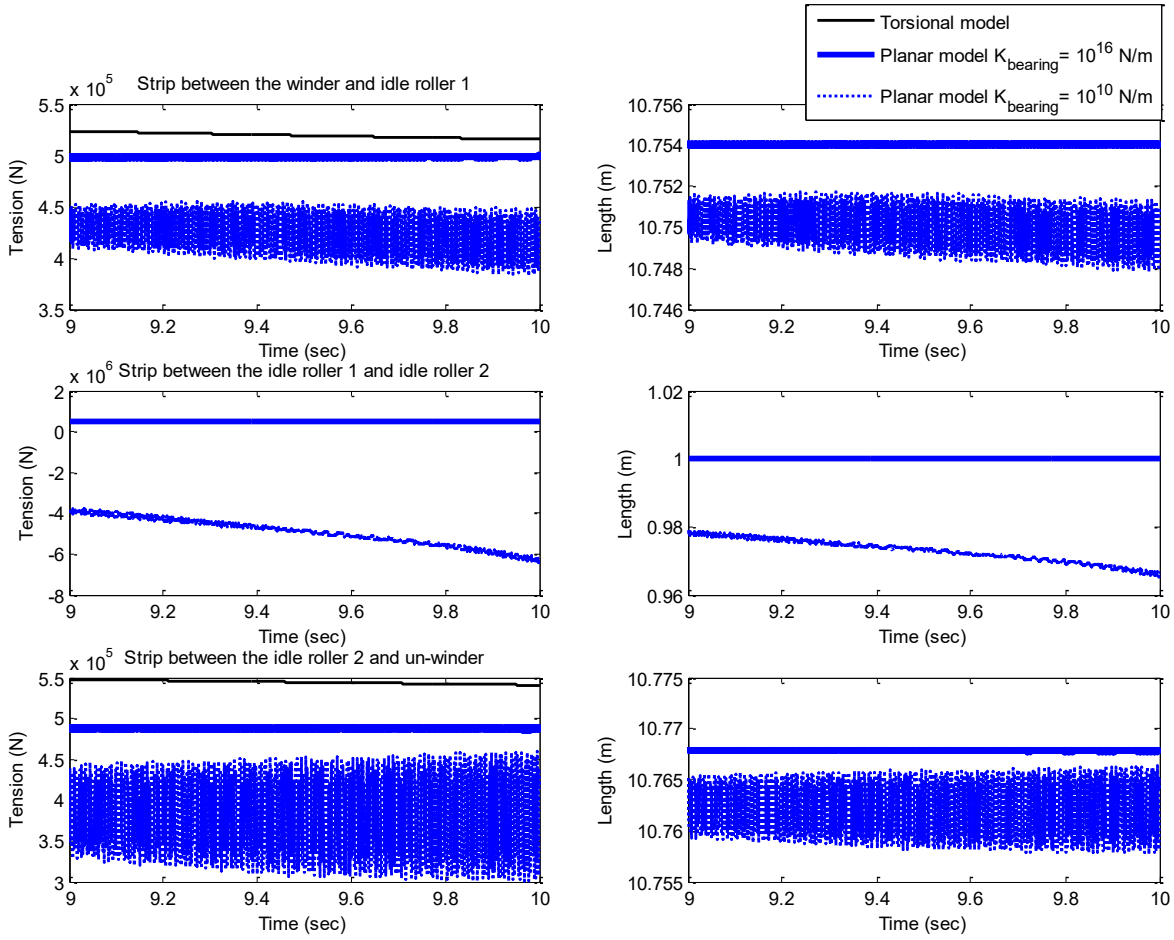

Fig. 6. Tension and length variation of the strip span

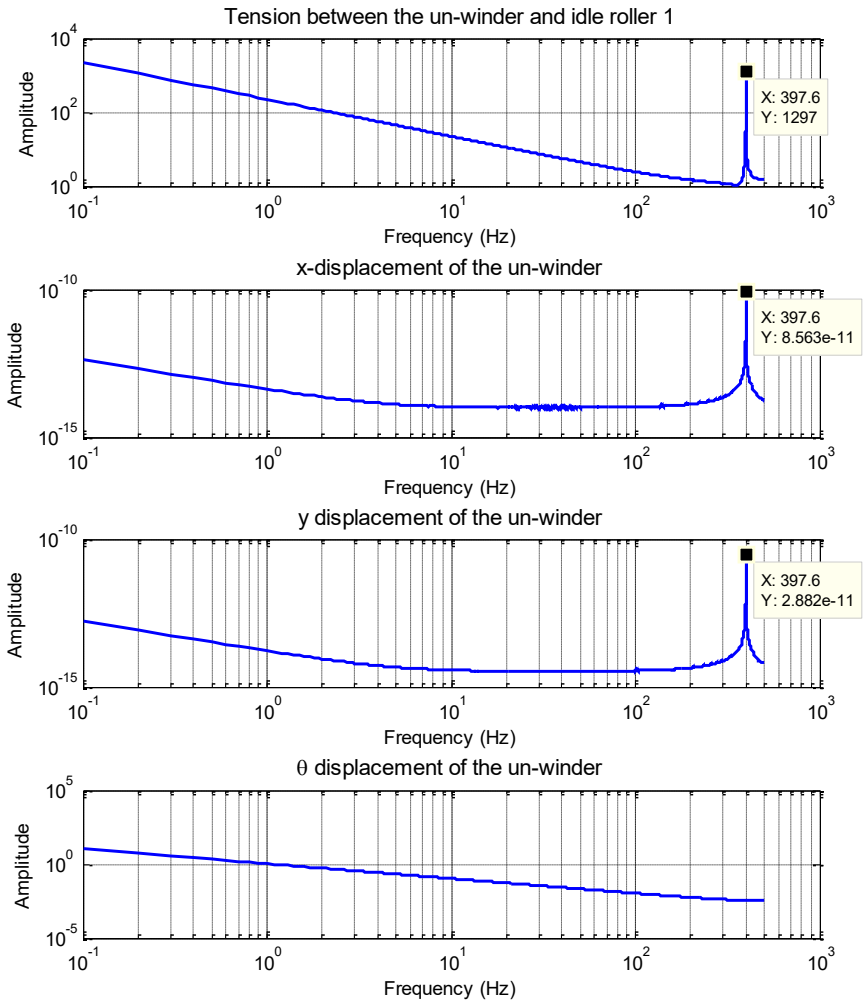

Fig. 7. FFT of the tension and planar motions of the unwinder

4.2 Dynamic response according slip on the idle roller

When the strip does not slip, friction force on it is the same as on the roller, so to rotate the roller the motor torque need consider only the tension as set up. However, when the strip does slip, the friction is the same as the strip tension without slip. However, some peak frequencies occur in the Fourier transform (Fig. 8). We defined the magnitude of the friction on the idle roller to be 90 % of the strip tension; so to maintain constant rotation the torque motor should compensate for 10 % of the torque difference. The peak frequency was 31.4 Hz, but the frequency changed with the magnitude of the friction. For instance, the peak frequency was 4.5 Hz when the magnitude was 99.99 %, and 44.4 Hz when the magnitude was 80 %. Compared to the bearing stiffness, the peak frequency appears at lower frequency, and coupled peak frequency did not happen except for some transient responses.

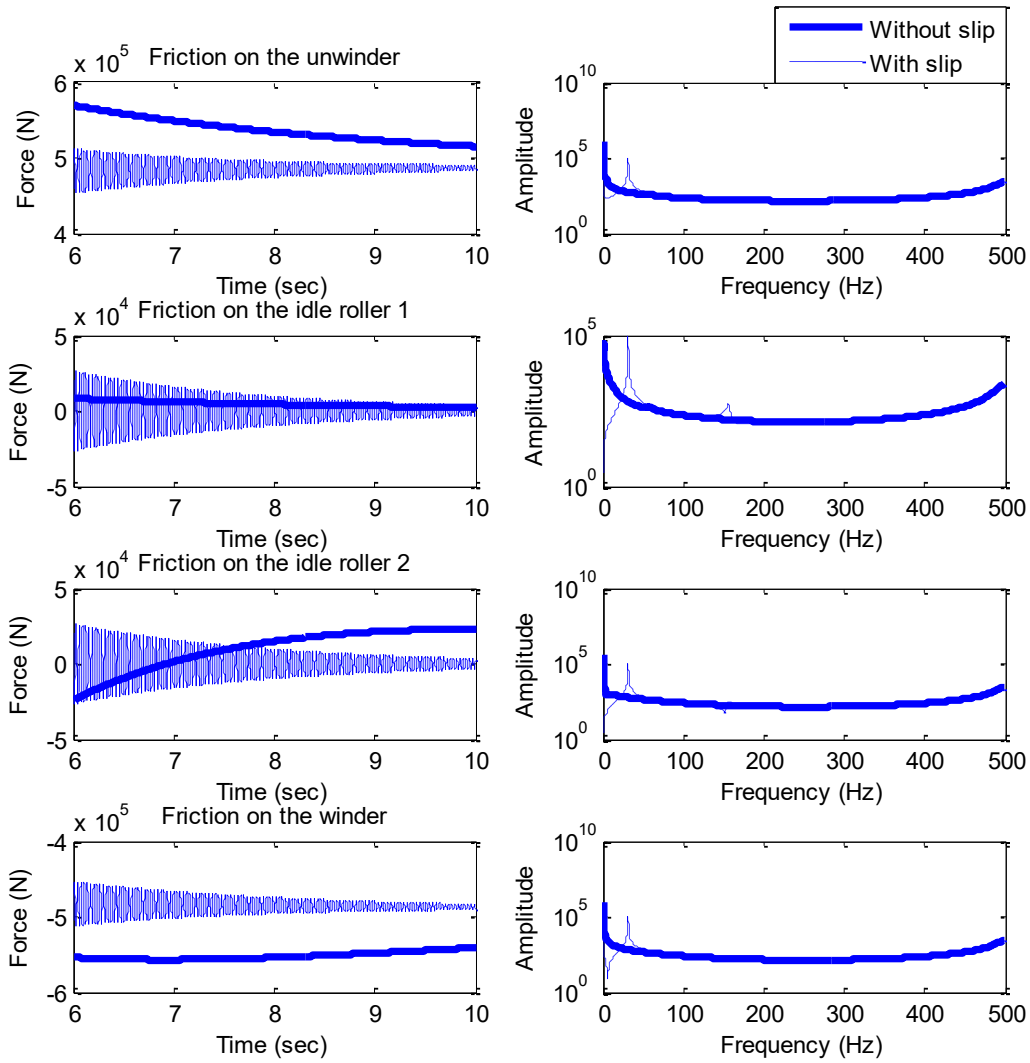

Fig. 8. Time history & FFT of friction on the unwinder, idle rollers, and winder

4.3 Dynamic response according eccentric problem

The eccentric mass affected the planar motions of the rotary directly. If irregular planar motions occur at the unwinder (i.e. a relative rotary component), the idle roller is also affected as a result of the stiffness of the strip. Therefore, the effect of this phenomenon on the angular velocity of the rotary with eccentricity must be determined. The eccentric unwinding problem was pre-defined about a 0.2-m moment arm, and the results were subjected to Fourier transform (Fig. 9). The major differences between the models occurred at 2.400-Hz and 2.599-Hz peak frequencies. To investigate their physical meaning, we represented the peak frequency as

$$\text{Frequency} = \frac{\text{V}}{\text{r}_{\text{ecc}}} = \frac{200/60[m/s]}{0.2120\,m}\frac{1}{2\pi} = 2.502\,\text{Hz} \tag{17}$$

which is similar to the observed values in Fig. 9.

Based on this result, we checked the roller real time using

$$\frac{V_{current}}{r_{outer}} \leq \text{Peak frequency} \leq \frac{V_{current}}{r_{inner}} \tag{18}$$

to determine whether the peak frequency occurred in a specific frequency range.

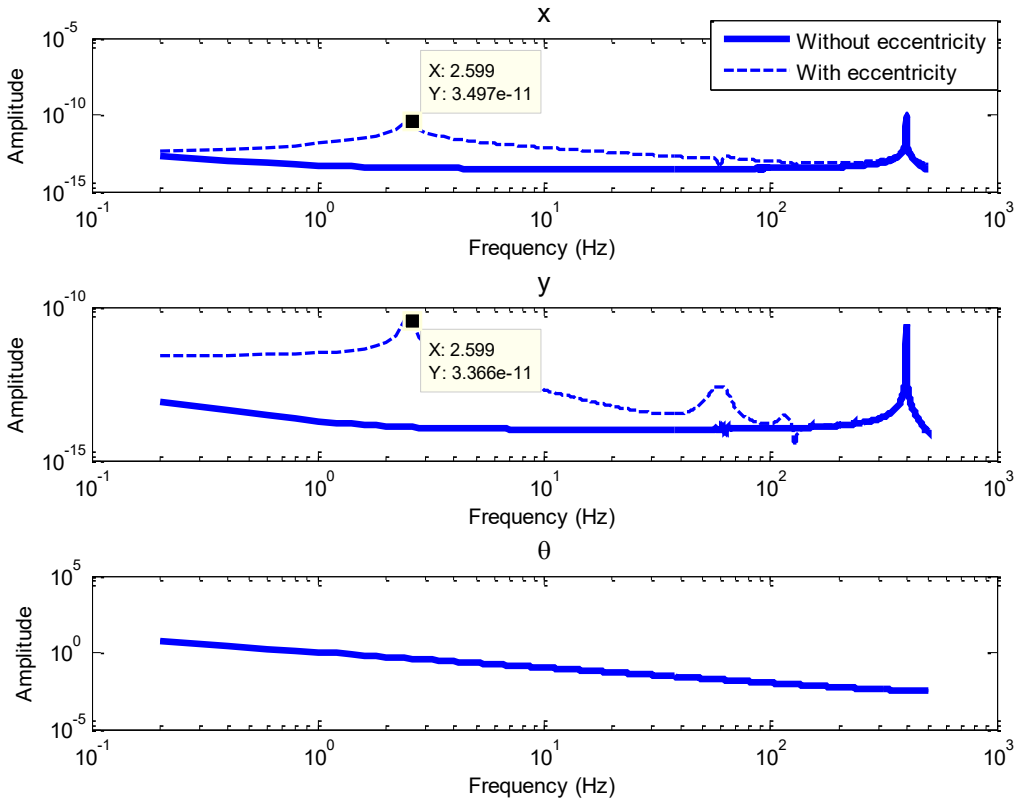

Fig. 9. FFT of the planar motions of the unwinder

4.4 Dynamic responses with pre-tension for the coil

Compared to the strip tension of 50 tons, the pre-tension required to shape the coil is trivial (92.6 N), because this model is only valid until strip layers start to contact each other. After that, the over-compressive winding mechanism cannot be expressed. However, we found that the

physical qualities of the unwinder and winder varied in the same way with winding radius (Fig. 10). These physical quantities represent the strip statue, and can be checked by operating conditions whether the winding operates properly or not.

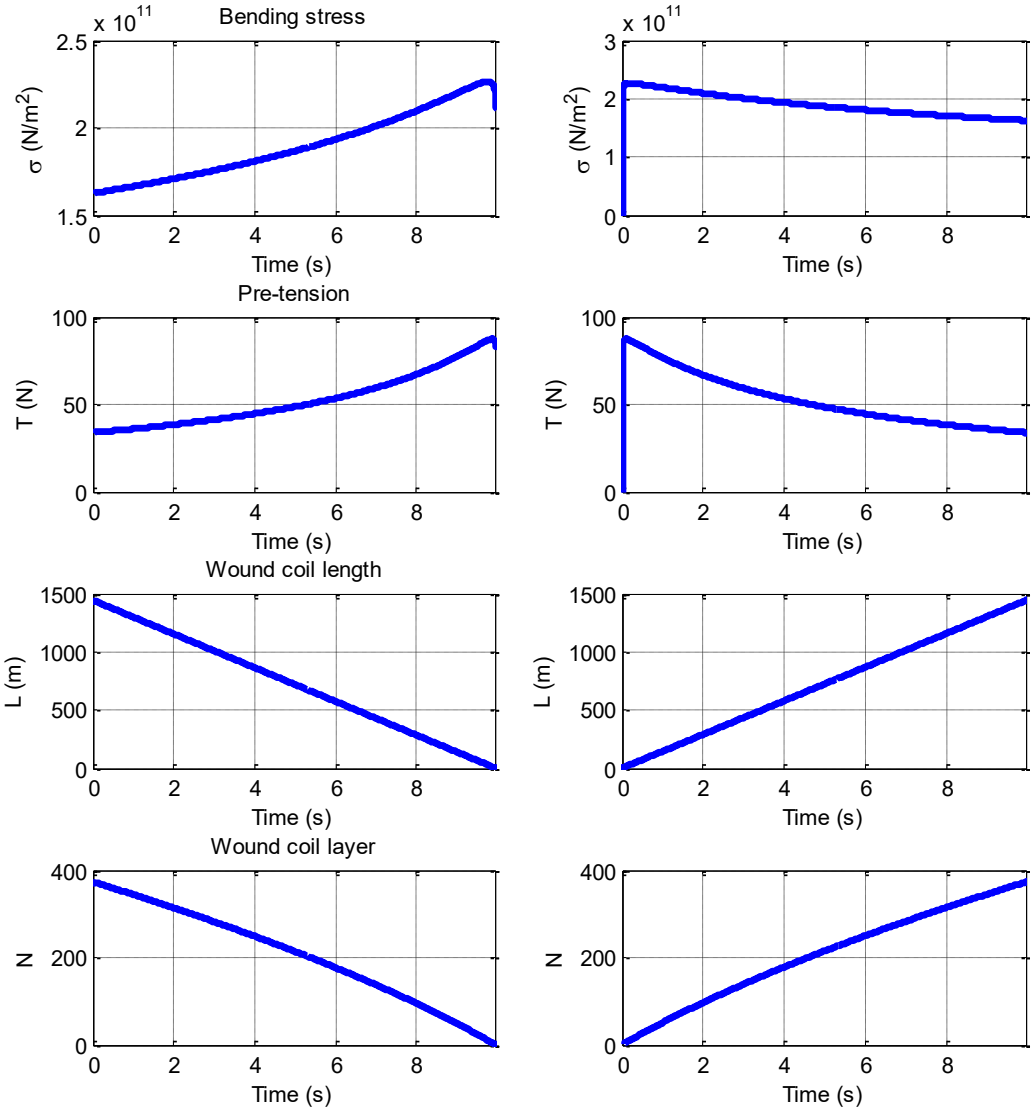

Fig. 10. Dynamic response of the unwinder (L) and winder (R) including the pre-tension

5. Conclusion

We investigate a mathematical model of a winding system that includes a submodel of the unwinder-idle roller-winder for the steel strip; this submodel was taken from a previous web model. Considering that bending resistance and restoring force of the strip is much higher than that of the web, we expand the model with planar motions that include bearings, eccentricity, and pre-tension to maintain the coil shape. In contrast to the previous model, we used by using a Taylor's series to calculate a non-linear property that comes from geometrical variation. We also developed automatic code to calculate a contact point and the tangential velocity of the strip. Through dynamic responses, the bearing status is a very important factor that affects both its rotary behavior and the strip tension. A Fourier transform revealed additional peak frequencies: the bearing imposes its natural frequency on the strip tension, slip causes a single low-frequency peak on the friction, and eccentric rotation causes a peak frequency in the planar motions that correspond to the angular velocity of rotation.

However, our model has a limit that relationship between the strip and roller is too simple to represent tighten and untighten of the strip coil in detail. Also, the pre-tension model cannot predict over-compressive coil state. We plan to remedy this demerit by using numerical analysis of a thick cylinder and a finite element winding model to develop a detailed mathematical model of a wound coil, and then combining it with the present model.

Acknowledgments

This work was supported by the POSCO Research Project (2015Y011) from POSCO Engineering solution center, and the Korea Institute for Advancement of Technology (KIAT) grant funded by the Korea Government Ministry of Trade Industry and Energy (MOTIE). (2015 Establishment of GEM, No. H2001-13-1001)

Reference

[1] Kang, H. S., Hong, W. K., & Hwang, I. C. (2012). Modeling and State Observer Design for Roll Slip in Cold Cluster Mills. Transactions of the Korean Society of Mechanical Engineers A, 36(12), 1543-1549.

[2]. J. M. Koo, H. J. Kim, J. K. Lee and S. M. Hwang (2003). Residual Stress Analysis of Hot Rolled Strip in Coiling Process. Transactions of Materials Processing, 12(4), 302-307

[3] K. C. Park, J. B. Nam (2012). A Study on the Effect of Sheet Properties and Coiling Conditions on the Sheet Shape by Deformation Analysis for Coiling. Proceedings of the Korean Society for Technology of Plasticity Annual Conference, 255-258

[4] Y.J. Jung, G.T. Lee, and C.G. Kang (2002). Tension/Heat/Thermal Deformation Analysis of a Cold Coiled Strip in Coiling Process. Proceedings of the Korean Society for Technology of Plasticity Annual Conference, 39-43

[5] K. T. Park, Y. H. Park, K. S. Kim, S. Y. Won, W. K. Hong, M. S. Chun, H. C. Park. (2015), Identification of mechanism and development of finite element analysis model for cold rolled strip coiling process, Annual conference of the Korean Society of Mechanical Engineers, Je-ju, korea, 10-14, November

[6] Brandenburg, G. (1976, May). New mathematical models for web tension and register error. In Proceedings of the 3rd International IFAC Conference on Instrumentation and Automation in the Paper, Rubber and Plastics Industries (pp. 411-438).

[7] Shin, K. H., Reid, K. N., & Kwon, S. O. (1995). Non-interacting tension control in a multi-span web transport system. In Proceedings of the third international conference on web handling (pp. 312-325).

[8] Pfeiffer, J. D (1977). Nip forces and their effect on wound-in tension [Paper production]. Tappi.

[9] KYU TAE, KIM (1997). A Nonlinear PID Control of the Winding Tension Using a Contact Roll. Master thesis, Mechanical Design and Production Engineering Graduate School of Kon-Kuk University

[10] Gaby Saad (2000), MULTIVARIABLE CONTROL OF WEB PROCESS, Master thesis, University of Toronto

[11] Koc, H., Knittel, D., De Mathelin, M., & Abba, G. (2002). Modeling and robust control of winding systems for elastic webs. Control Systems Technology, IEEE Transactions on, 10(2), 197-208.

[12] F. Beer and E. Johnston (1992), Mechanics of Materials. McGraw Hill, New York

[13] Hee-Chul Yang (2009). A Study on Exposure System for Flexible Printed Circuit. Master thesis, Department of Mechatronics Engineering in Graduate School of Tongmyong University

[14] Yong-Hwan Kim (2010). A Study on Tension Control of Roll to Roll System with Flexible Substrate. Master thesis, Department of Mechanical System Engineering in Graduate School of Tongmyong University

[15] Whitworth, D. P. D., & Harrison, M. C. (1983). Tension variations in pliable material in production machinery. Applied Mathematical Modelling, 7(3), 189-196.

[16] Rao, S. S., & Yap, F. F. (1995). Mechanical vibrations (Vol. 4). Reading: Addison-Wesley.

[17] Changwoo Lee (2014). Effect of Taper Tension Profiles on Radial Stress of a Wound Roll in Roll-to-Roll Winding Process. J. Korean Soc. Precis. Eng., 31(2), 125-131

[18] Mechanical, Industrial and Technical Calculations (2014), “Spiral springs”, http://www.mitcalc.com/doc/springs/help/en/springs.htm (accessed May 6, 2015)